TRANSPORTATION LEARNING NETWORK

A partnership with MDT•NDDOT•SDDOT•WYDOT and the Mountain-Plains Consortium Universities

Welcome!

DURABLE BRIDGES USING GLASS FIBER REINFORCED POLYMER AND HYBRID REINFORCED CONCRETE COLUMNS

Presented by: Chris P. Pantelides

Our partners:

Mountain-Plains Consortium · Montana MDT Department of Transportation · North Dakota Transportation · SD Department of Transportation · Wyoming Transportation Department · NDSU · Upper Great Plains Transportation Institute, Transportation Learning Network

This material is subject to change at the discretion of the presenter. If there are changes, TLN will obtain a revised copy to be posted on the LMS for download after the presentation. Thank you.

Outline

- Introduction
- Proposed Research
- Pull-out Tests
- Non-Post Tensioned Column Experiments
- Post Tensioned Column Experiments
- Computational Study

Accelerated Bridge Construction (ABC)

- Quick construction time
- Superior quality of the prefabricated components
- Minimal interruption to traffic during construction, especially in densely crowded areas

Seismic Connections Investigated in ABC

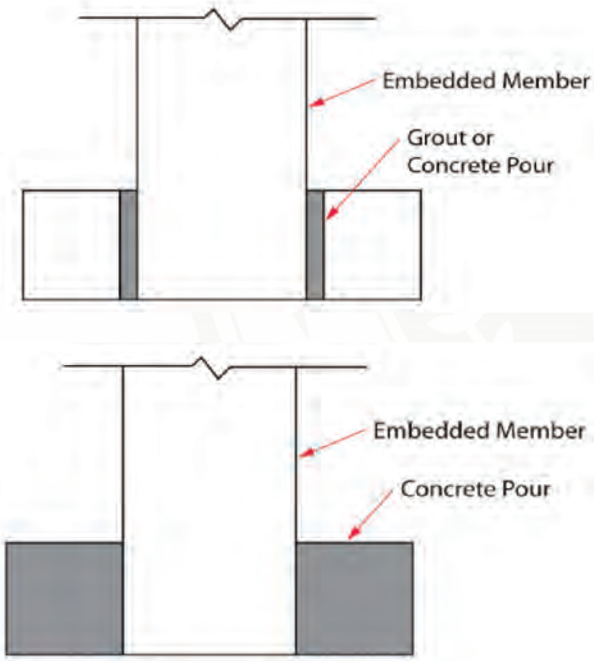

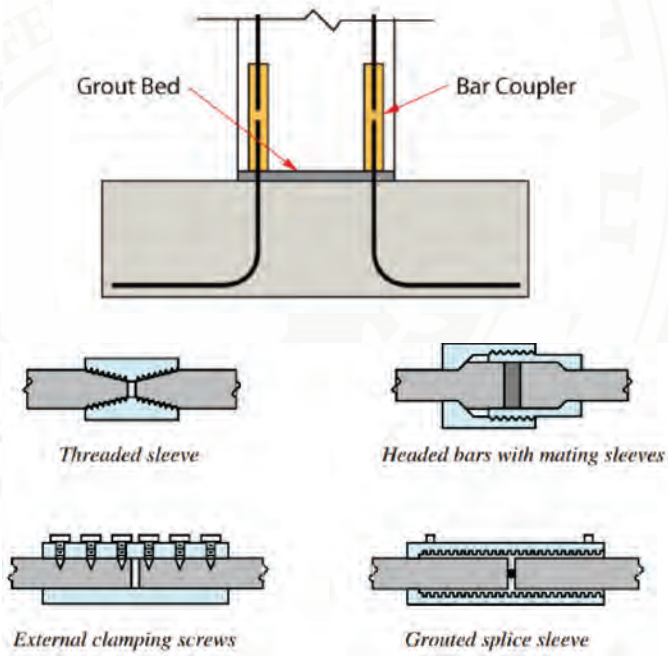

Socket Connections

Bar Coupler Connections

Seismic Connections Investigated in ABC

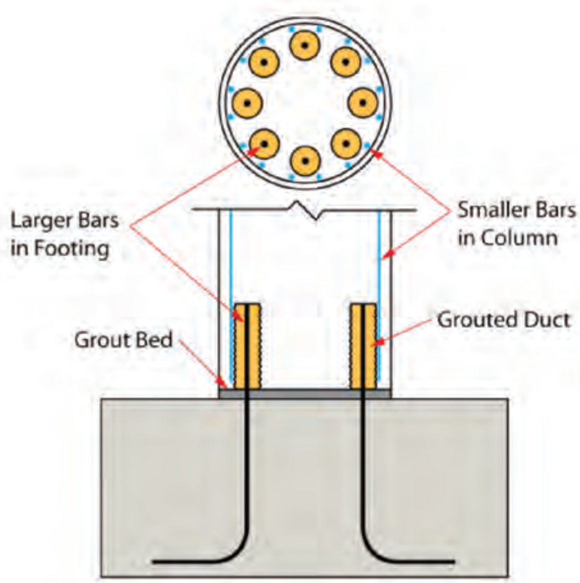

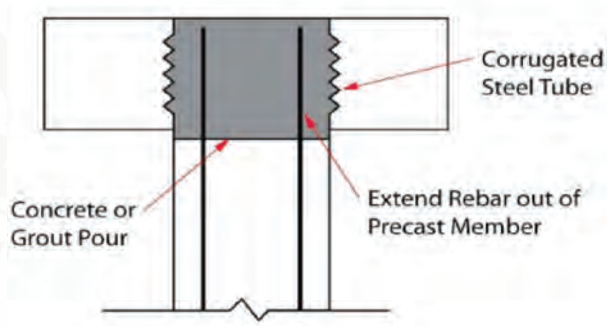

Grouted Duct Connections

Pocket Connections

Seismic Connections Investigated in ABC

- According to NCHRP Report 698: “Application of Accelerated Bridge Construction Connections in Moderate-to-High Seismic Regions (2011)”
  - *Socket Connections*, excellent performance, difficult to implement
  - *Pocket Connections*, acceptable performance, constructible
  - *Bar Couplers*, good performance, difficult to implement
  - *Grouted Duct Connections*, good performance, good constructability
- Reasons for picking Grouted Duct Connections:
  - *Material availability on the market:* popular, not depending on a specific manufacturer.
  - *Great tolerance for assembling:* thanks to largely varying duct diameter.
  - *Grout development:* self-developing, not depending on duct manufacturers
  - *Economical approach:* cost-saving to produce and transportation

Grouted Duct Connection

- Assembly: corrugated galvanized steel ducts embedded into one member with reinforcing dowels of another precast member inserted into the first component.
- Finishing work: the ducts are then filled with high-strength grout to finish the joint.
- Force transferring mechanism: the forces from the rebars are transferred into the surrounding filled grout to the outside of the ducts.
- Application: pile to pile cap, spread footing or pile cap to the column, column to cap beam, and splice between column or cap beam segments.
- Summary: promising for good constructability.

Grouted Splice Sleeve (GSS) Connectors

Fiber Reinforced Polymer (FRP)

- a composite material system made of fibers and resin.
- FRP rebars and stirrups provide significant merits over traditional steel,
  - non-corrosion,
  - high strength-to-weight ratio,
  - and ability to form in any shape or application.

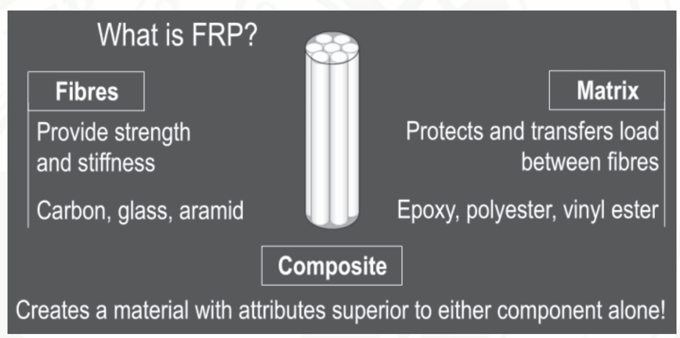

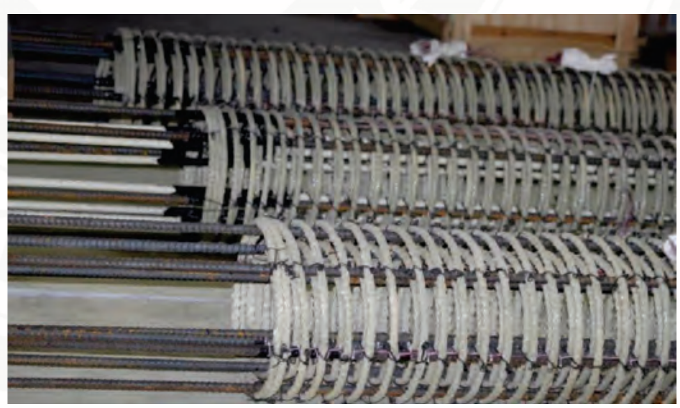

Fiber Reinforced Polymer (FRP)

- #6 Glass Fiber Reinforced Polymer (GFRP) Rebars

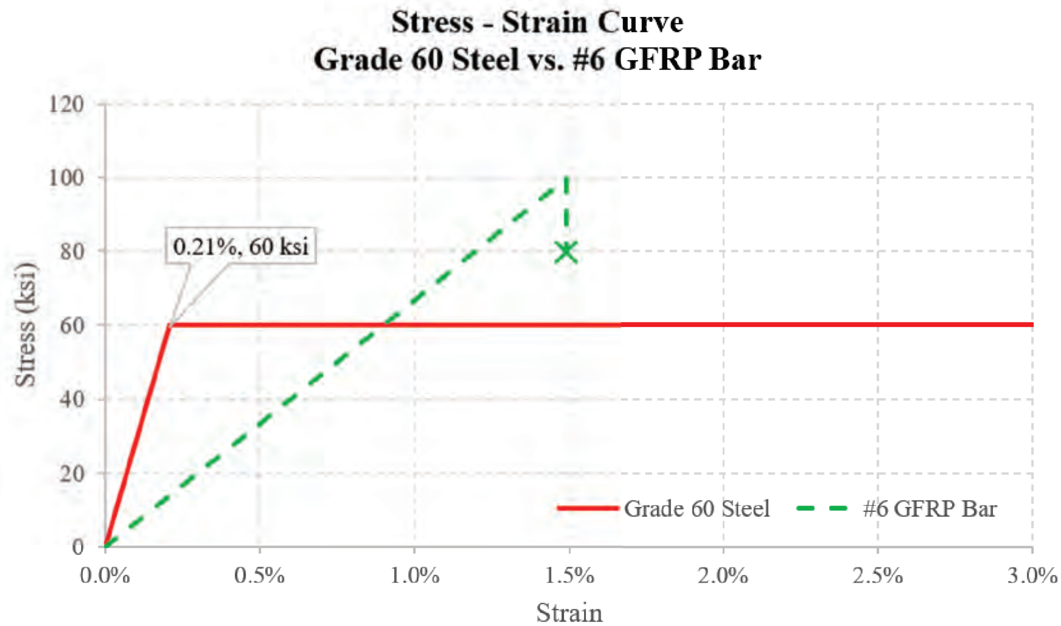

Post-Tensioned (PT) Bridge Bents

- Bents may have a Post-Tensioning system such as bar or strand post-tensioning systems.
- When the PT bar is unbonded, increased strain in the PT bar or strand is distributed over the whole length, which allows the bar/strand to remain elastic at large displacements and thus provide a restoring force to the basic large-bar system.

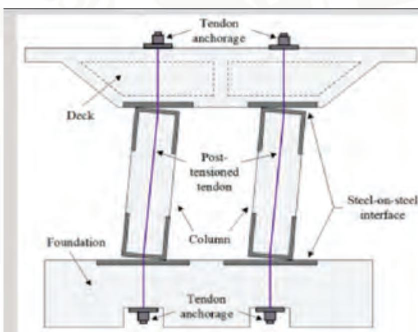

Zhou, Y.-L., et al. (2019)

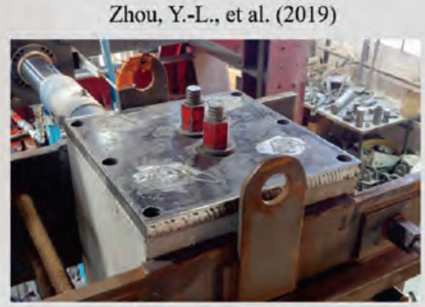

PT bars in current study

Research Gaps

- No information is available for the development length of GFRP bars in grouted ducts.
- Only a few references on the seismic performance of precast GFRP reinforced columns are available.
- No information on the seismic performance of hybrid (GFRP and steel reinforced) columns is available.
- No information on the seismic performance of hybrid columns incorporating PT for self-centering effect is available.
- No information on the seismic performance of steel/hybrid columns confined with double layers of GFRP spirals is available.
- No information on the modeling analysis of all specimen types listed above is available.

Proposed Research

- This research proposes an ABC bridge approach of corrosion-resisting bridges with the self-centering capability to substantially reduce permanent displacement using Ultra-High-Performance Grout (UHPG) ducts.
- Non-PT group: two specimens with no post-tensioning columns and footings are investigated to assess the hybrid reinforced system's seismic performance using conventional steel and GFRP reinforcement.
- PT group: two additional post-tensioned column specimens are investigated; post-tensioning is achieved using all-threaded prestressing bars to improve self-centering effectiveness using the exact reinforcement configuration as the non-PT specimens.

Proposed Research – Non-PT Columns

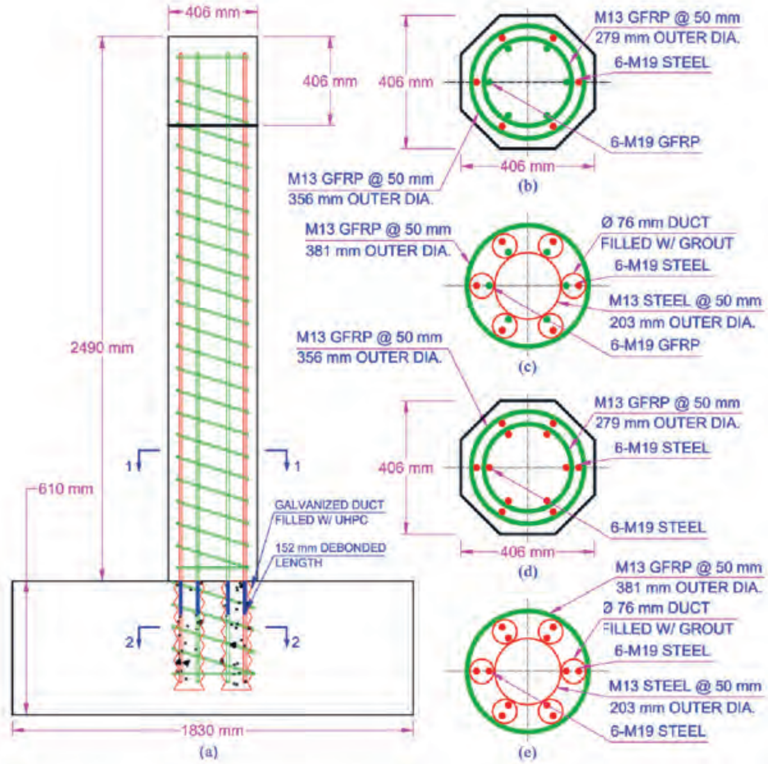

Introduction | Proposed Research | Pull-out Test | Non-PT Tests | PT Tests | Numerical Study

Proposed Research – PT Columns

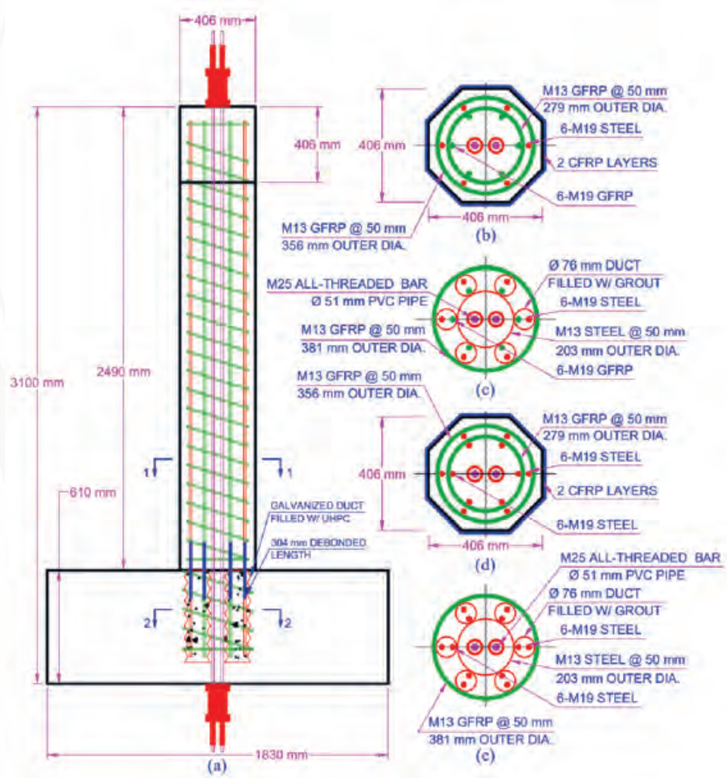

Introduction | Proposed Research | Pull-out Test | Non-PT Tests | PT Tests | Numerical Study

Pull-out Tests - GFRP #6 Bars in Grouted Ducts

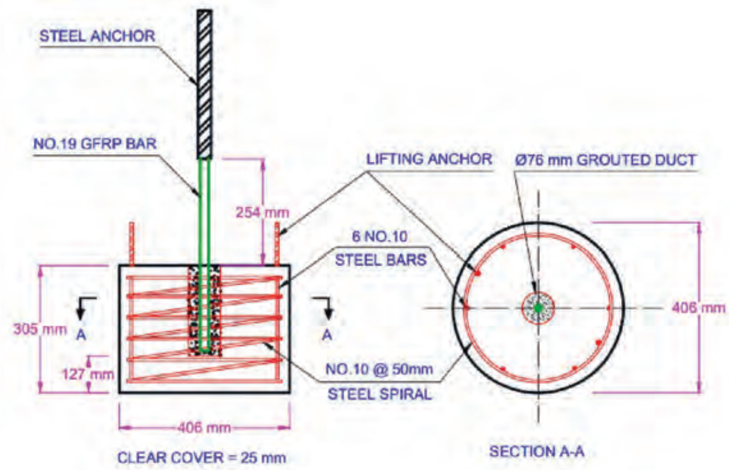

Ultra High Performance Grout

Material	Specific Gravity	Weight		Volume	
		(kg)	(lbs)	(m^3)	(ft^3)
Sand	2.59	43.98	96.97	0.01680	0.60
Silica	2.2	2.66	5.87	0.00120	0.04
Cement	3.15	15.08	33.25	0.00474	0.17
Water	1	5.32	11.74	0.00527	0.19
		Total Volume:		0.028	1.00

Note: Dosage of 15.6 liters of water-reducer per 100 kg of cementitious materials

Compression strength	7 days	28 days	35 days
Cylinder of 4x8 (in.)	7,700 psi	10,600 psi	11,800 psi

Failure Modes of GFRP #6 Bars in Grouted Ducts

Bar pull-out

Bar fracture

Bar fracture

Bar fracture

Non-PT Specimen Configurations

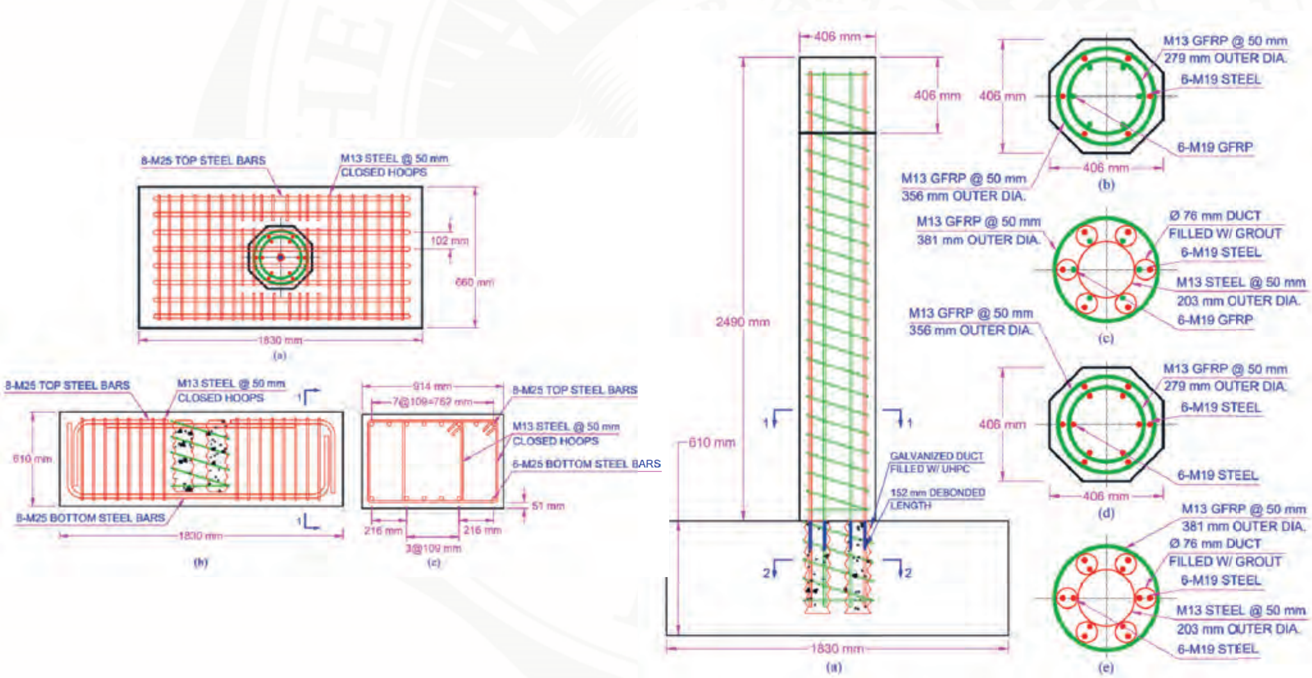

Non-PT Specimen Configurations

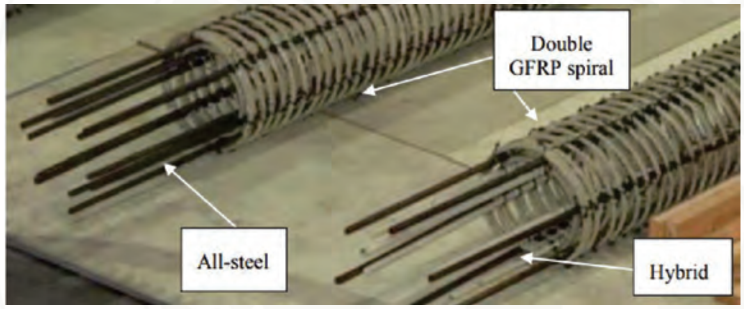

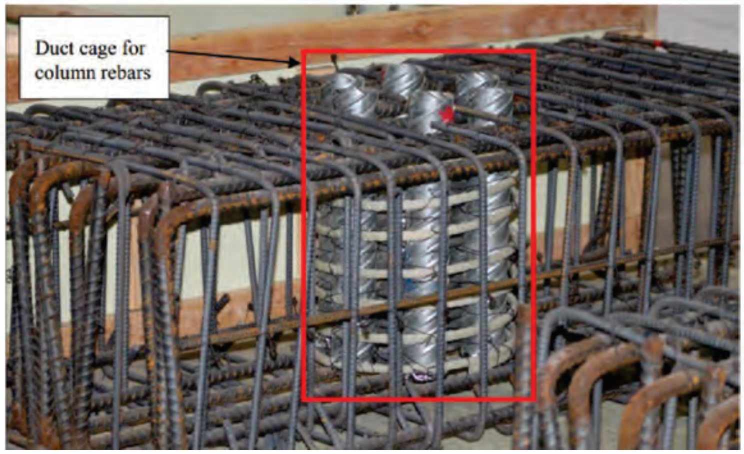

Introduction | Proposed Research | Pull-out Test | Non-PT Tests | PT Tests | Numerical Study

Test Setup

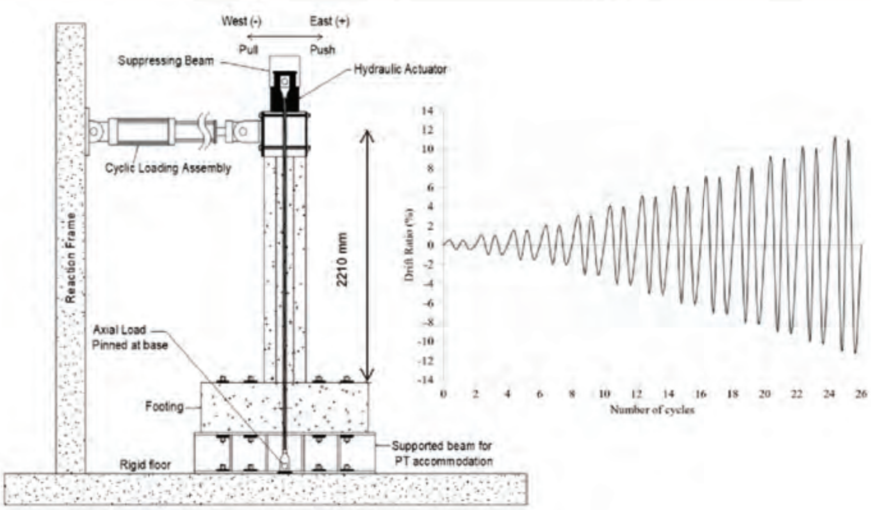

Introduction | Proposed Research | Pull-out Test | Non-PT Tests | PT Tests | Numerical Study

Hysteresis Performance

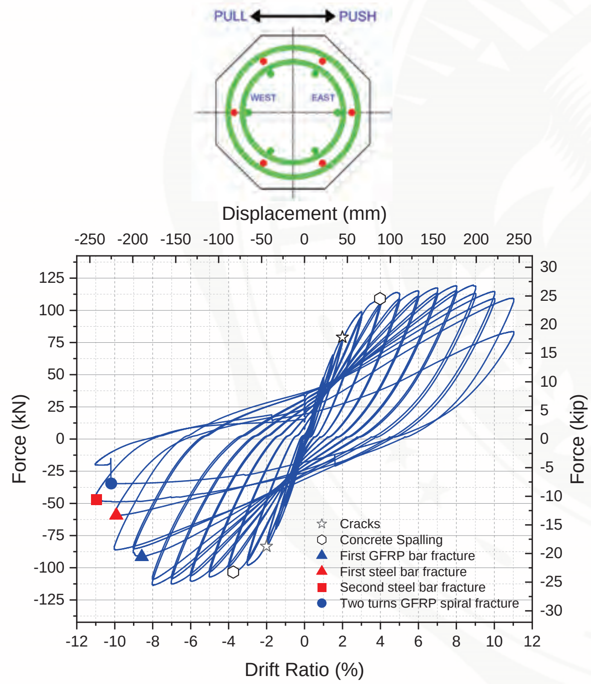

HYB

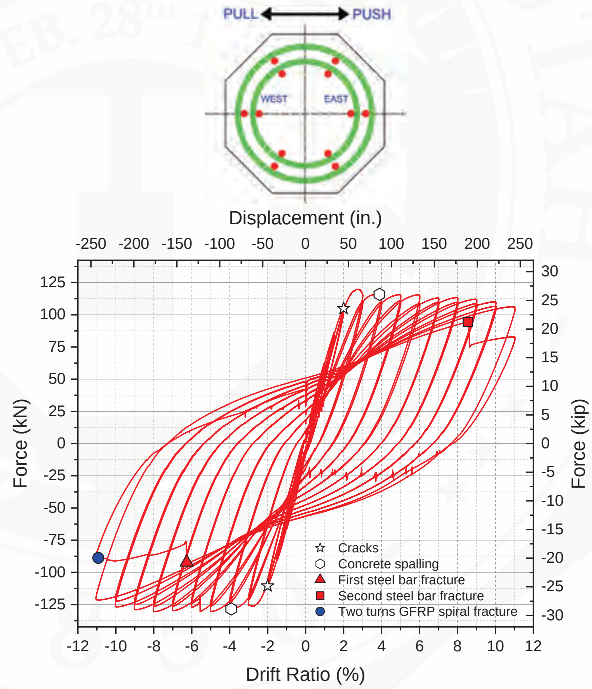

STL

Hysteresis Performance

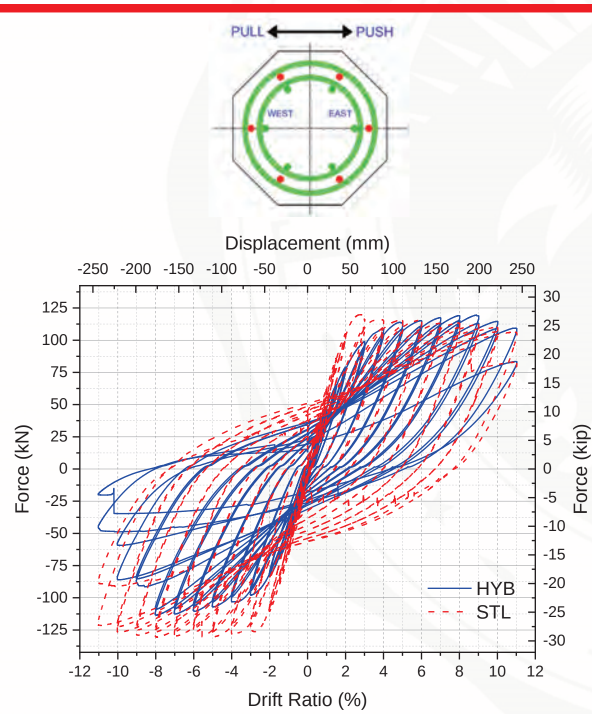

Hysteresis Comparison

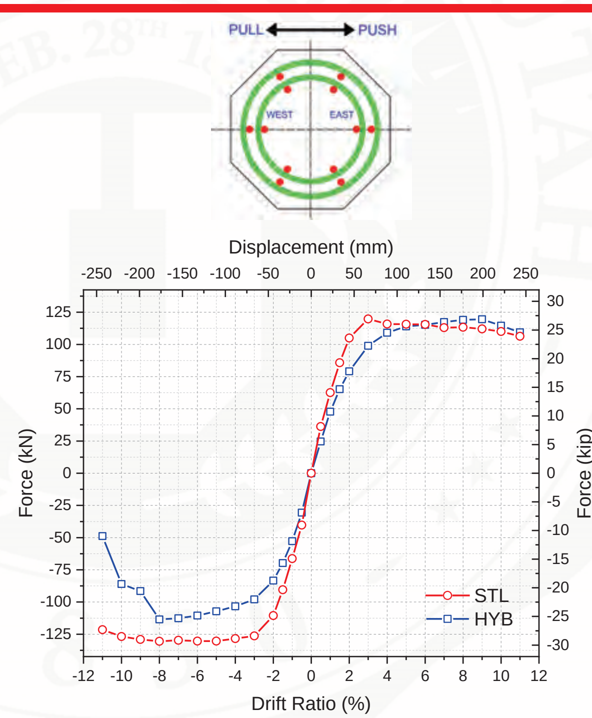

Hysteresis Envelope

Introduction | Proposed Research | Pull-out Test | Non-PT Tests | PT Tests | Numerical Study

HYB Column Failure

@ 6% drift ratio

@ 11% drift ratio

STL Column Failure

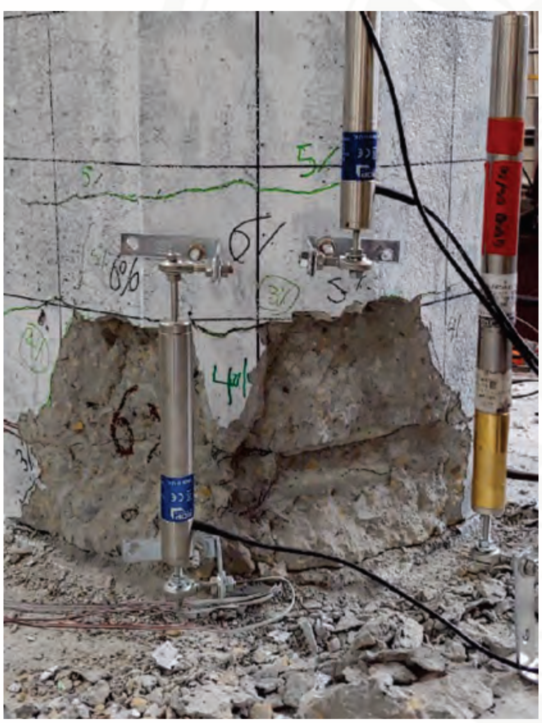

@ 6% drift ratio

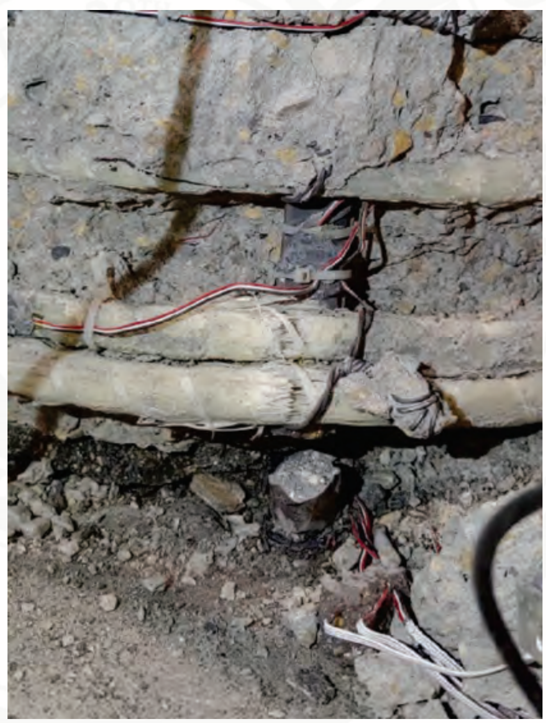

@ 11% drift ratio

Residual Displacement

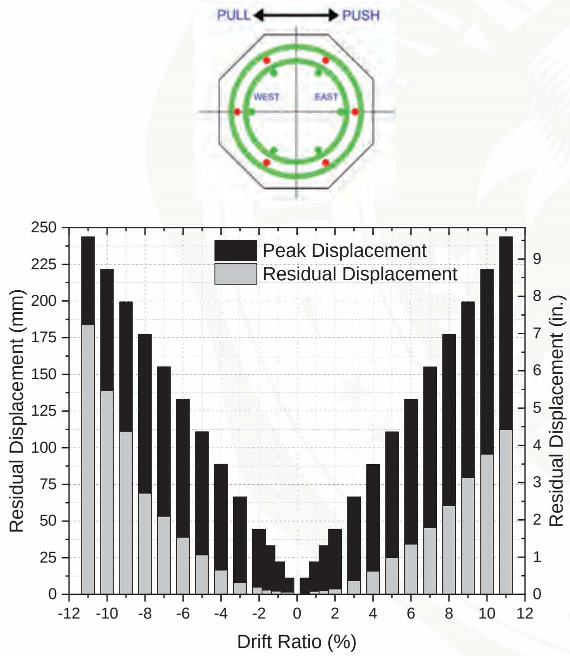

HYB

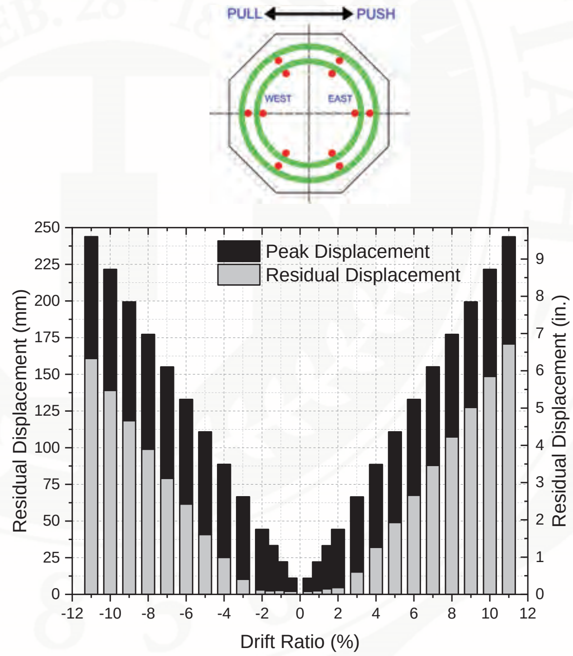

STL

Performance Comparison

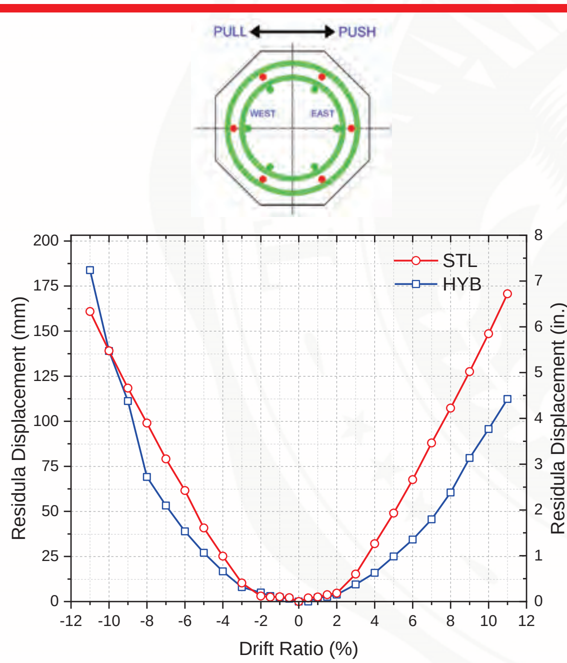

Residual Displacement

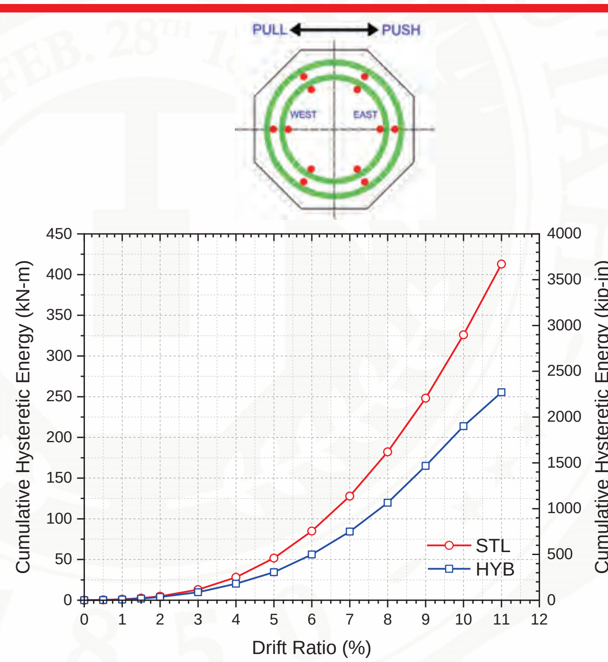

Hysteric Energy

Curvature Profiles

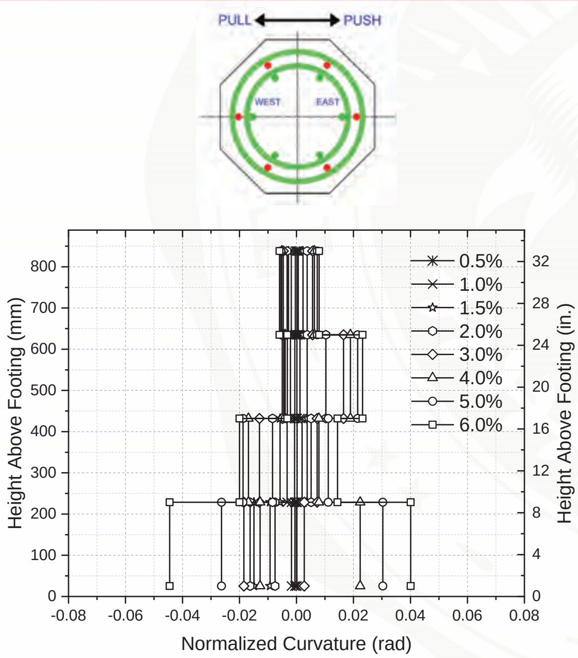

HYB

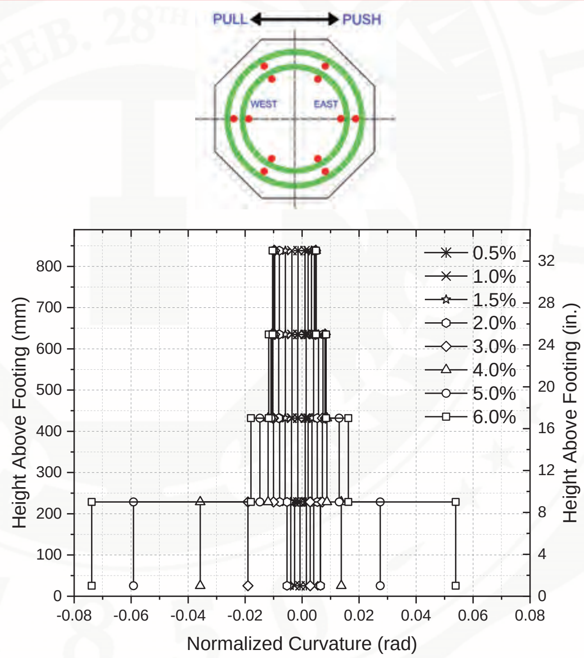

STL

HYB Strain Profiles

ε_y = 0.00234 (steel yield strain)

ε_u = 0.0149 (GFRP ultimate strain)

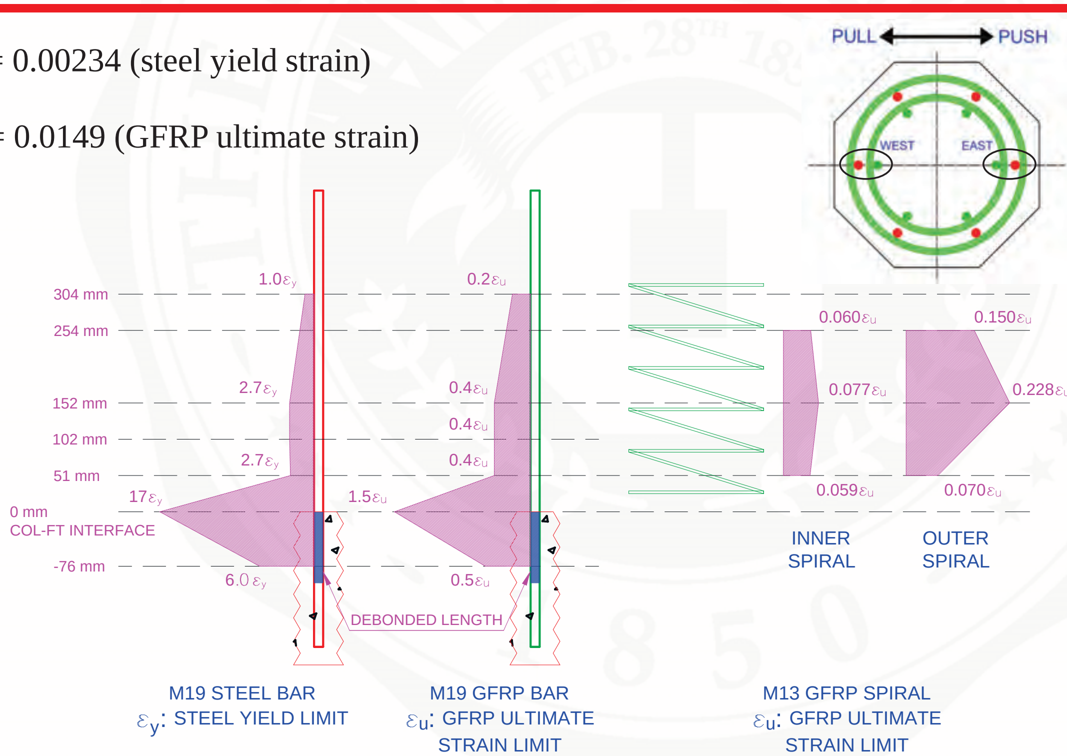

PT Specimen Configurations

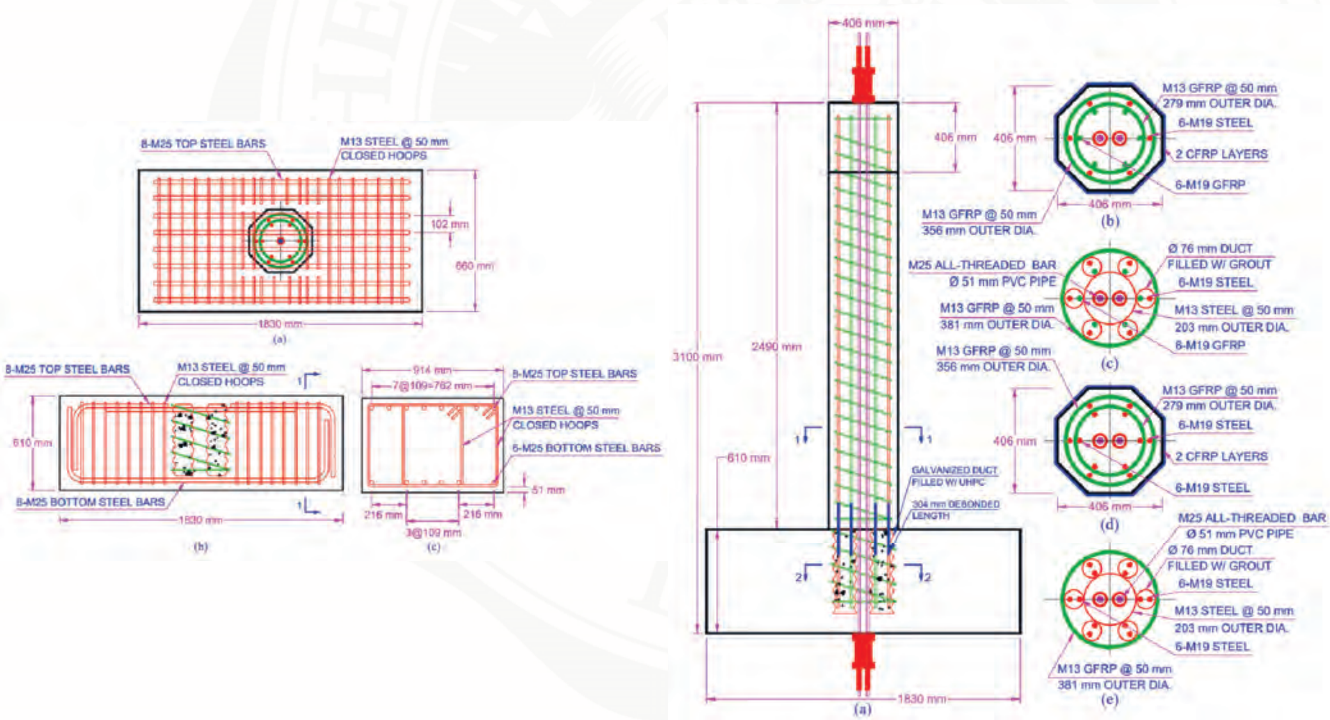

PT Specimen Configurations

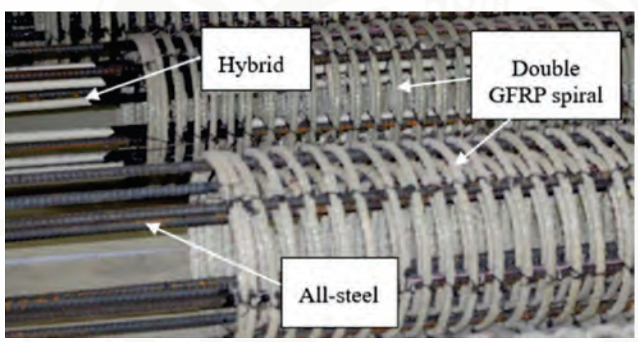

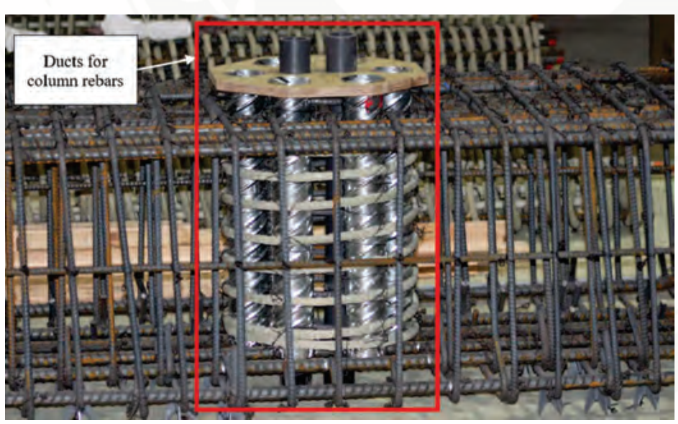

Test Setup

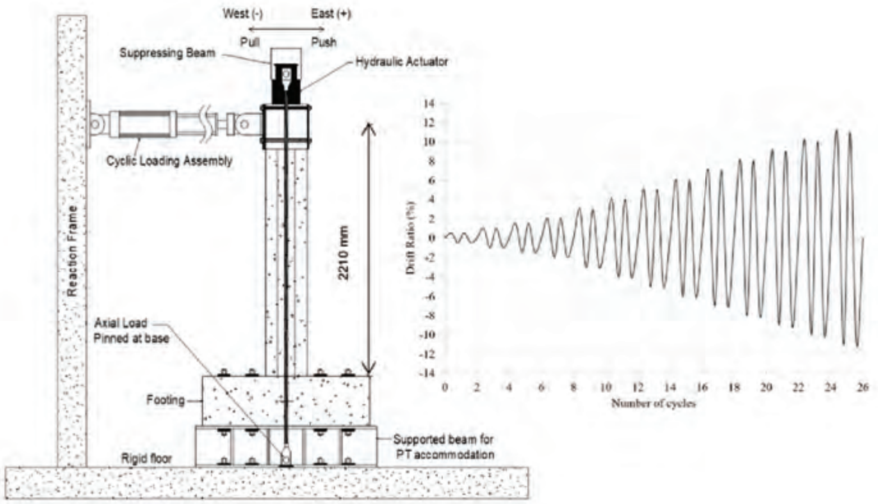

Hysteresis Performance

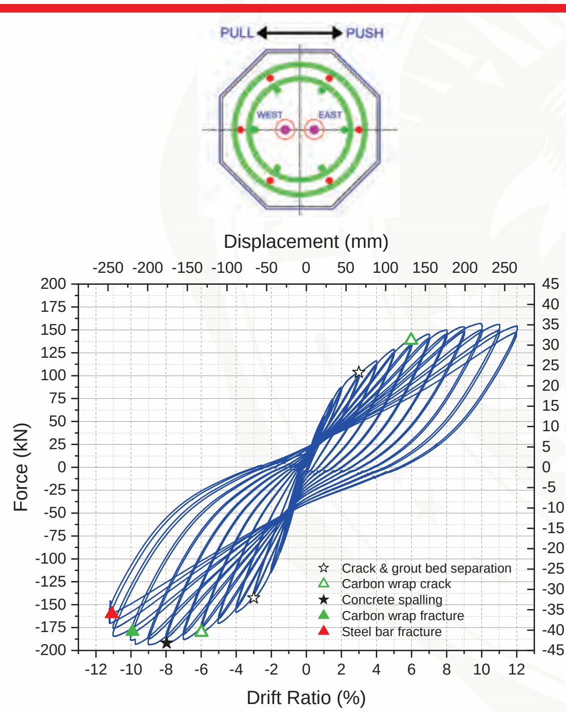

HYB

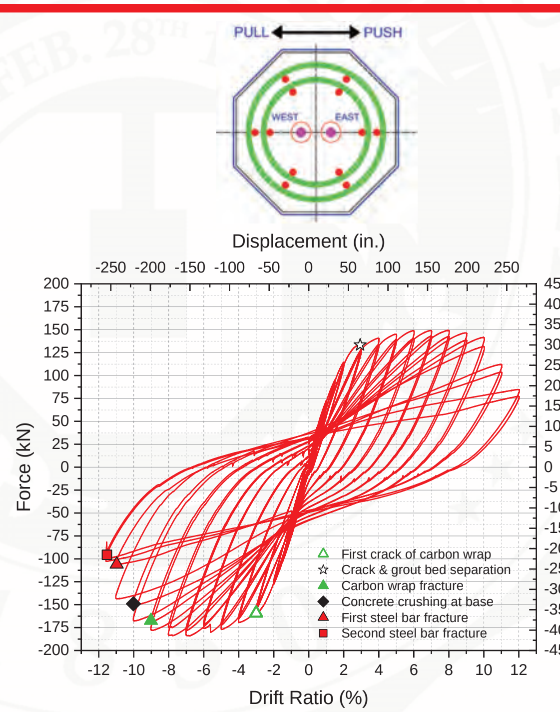

STL

Hysteresis Performance

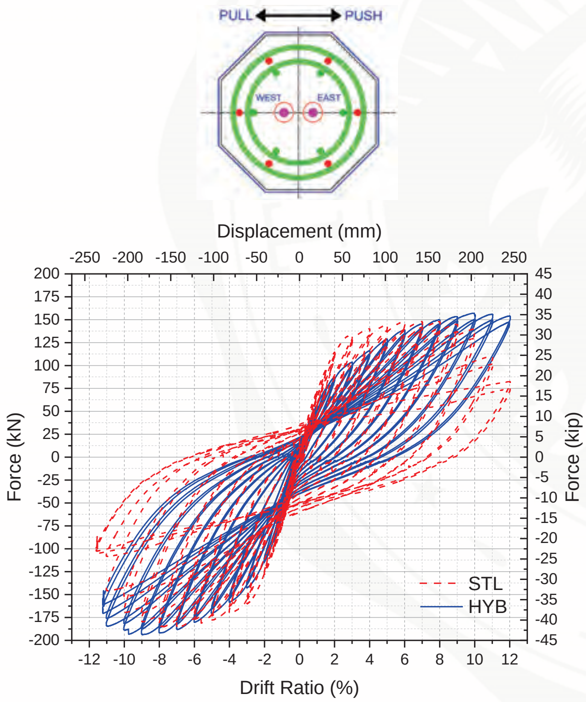

Hysteresis Comparison

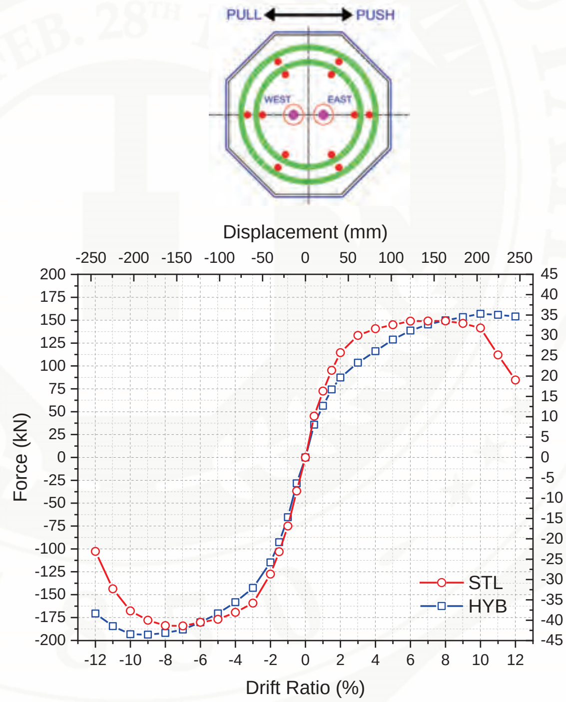

Hysteresis Envelope

Introduction | Proposed Research | Pull-out Test | Non-PT Tests | PT Tests | Numerical Study

HYB Column Failure

@ 11% drift ratio

@ 11% drift ratio

Introduction | Proposed Research | Pull-out Test | Non-PT Tests | PT Tests | Numerical Study

STL Column Failure

@ 11% drift ratio

@ 11% drift ratio

Residual Displacement

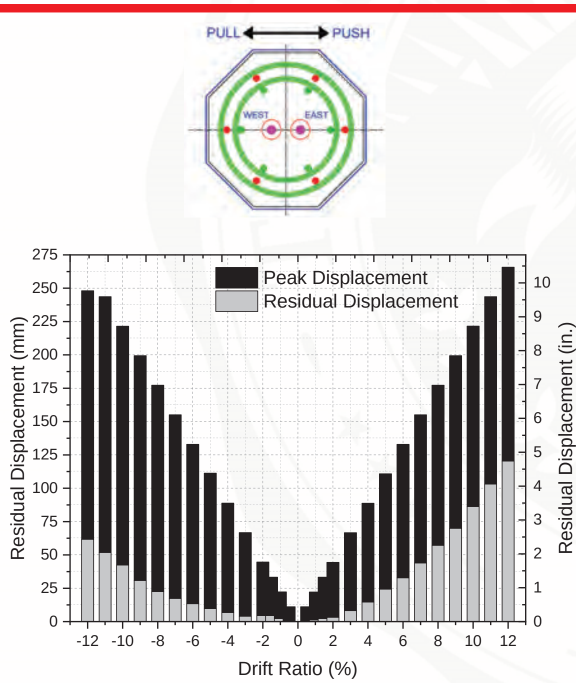

HYB

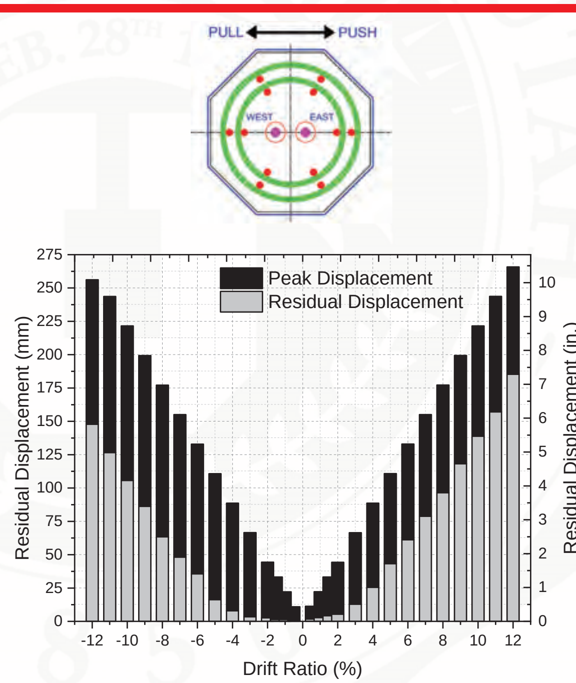

STL

Performance Comparison

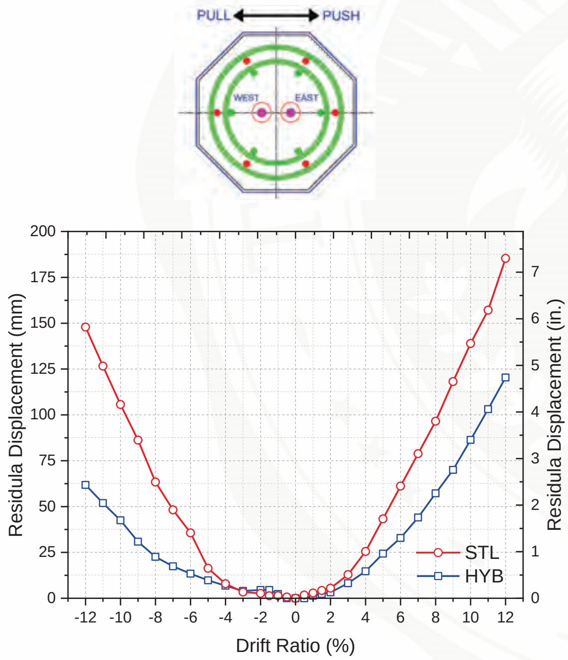

Residual Displacement

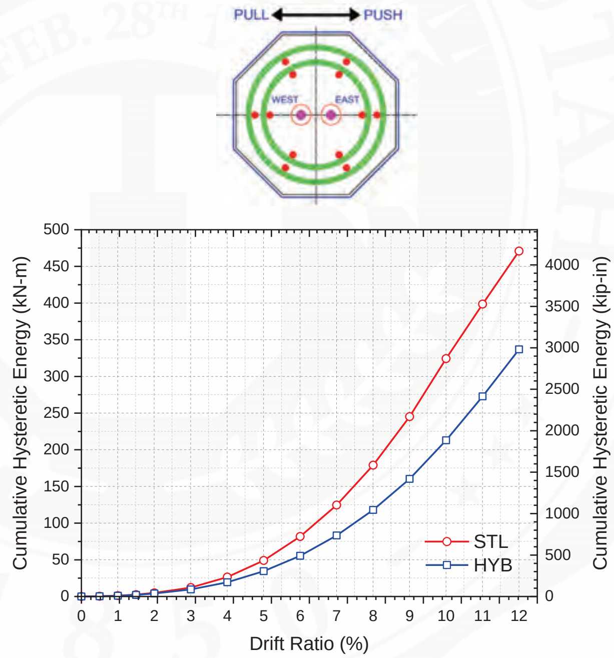

Hysteric Energy

PT Force Performance

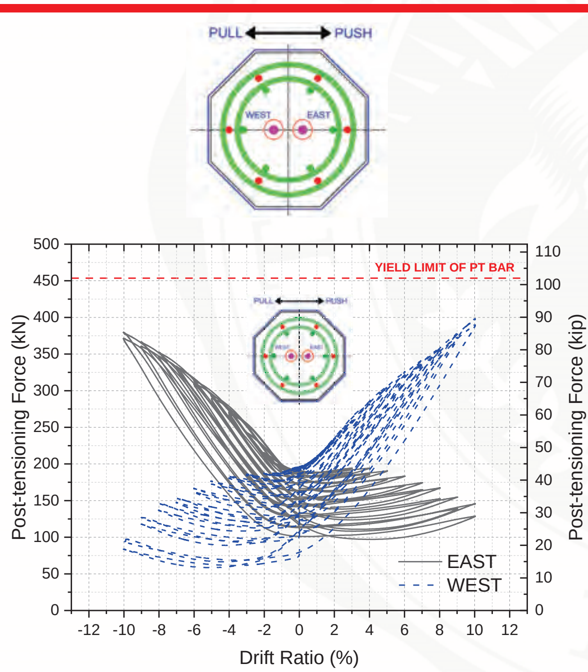

HYB

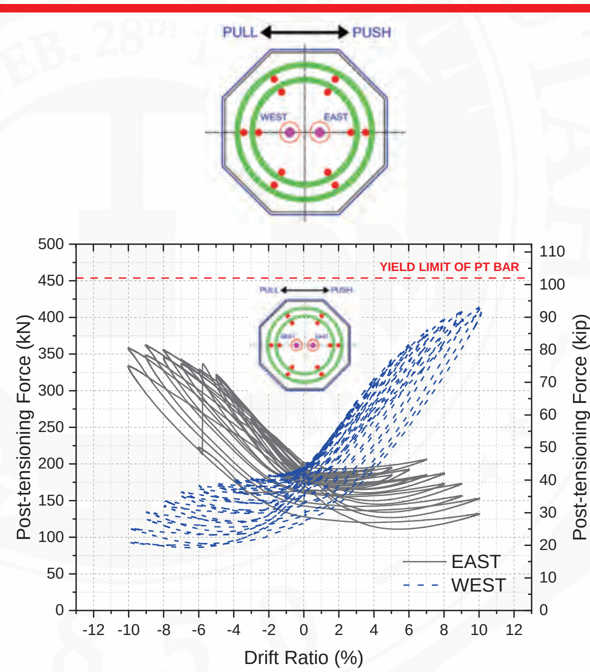

STL

Curvature Profiles

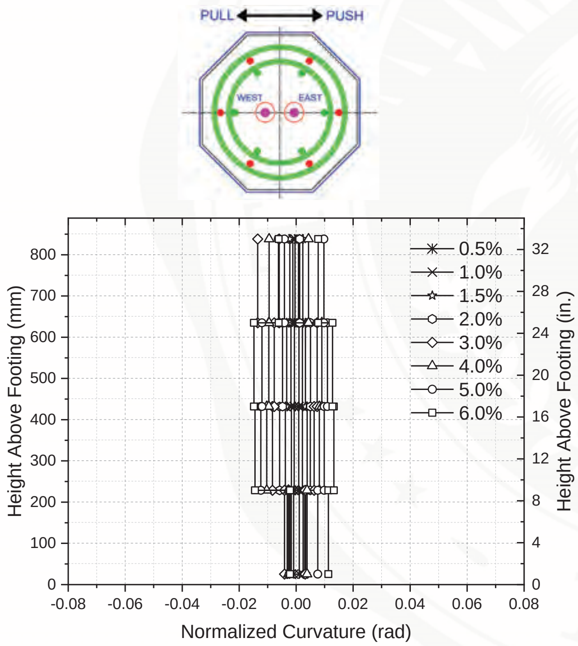

HYB

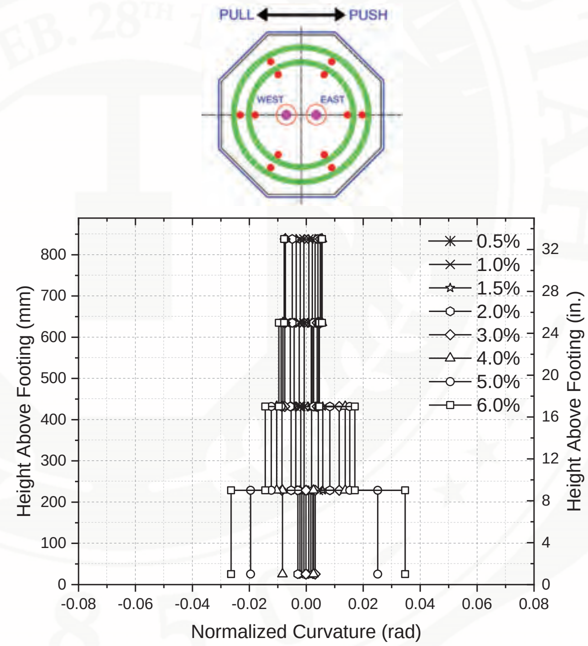

STL

HYB Strain Profiles

ε_y = 0.00234 (steel yield strain)

ε_u = 0.0149 (GFRP ultimate strain)

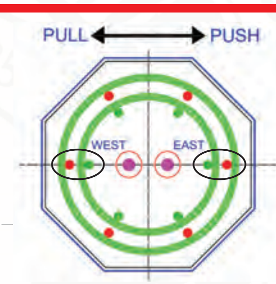

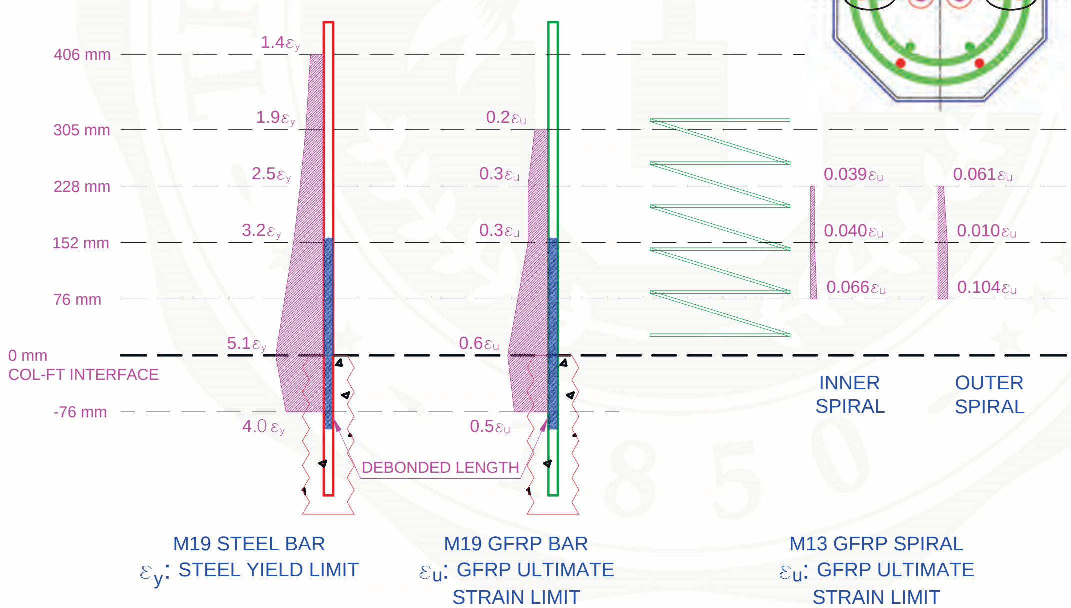

STL Strain Profiles

ε_y = 0.00234 (steel yield strain)

ε_u = 0.0149 (GFRP ultimate strain)

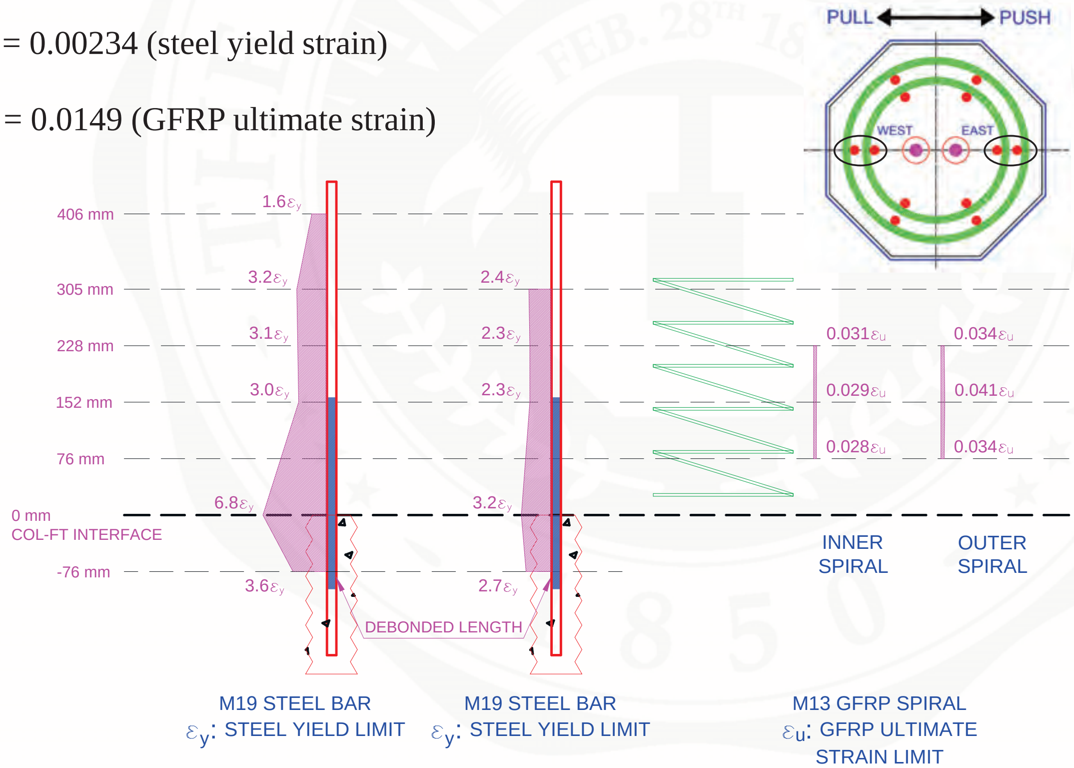

Numerical Objectives and Procedure

- Develop a predictive model capable of accurately simulating the seismic behavior of GFRP confined columns reinforced with all-steel or hybrid bars, both with and without a PT system.
  - Capable of accounting for differences between **mild steel** and **GFRP** rebars.
  - Includes softening effects of **bond-slip** (end rotation).
  - Capable of accounting for the **self-centering effect of PT bars**.
  - Capable of accounting for the **confinement effect of CFRP wraps**.
  - Includes different failure modes of **concrete crushing, GFRP bar fracture** and **low-cycle fatigue steel bar fracture**.
- The proposed model was validated with experiments through both global and local (sectional) responses.

Computational Modeling Tool

- OpenSees (Open System for Earthquake Engineering Simulation):
  - Open source software framework for finite element analysis
  - Versatile library of materials and elements, many of which are contributed
  - Materials available from simple bilinear to complex phenomenological models
  - Elements include beam-column elements and continuum elements
  - Python scripting language
  - More attractive in research than design

Validation Process

- Flowchart for validation process:

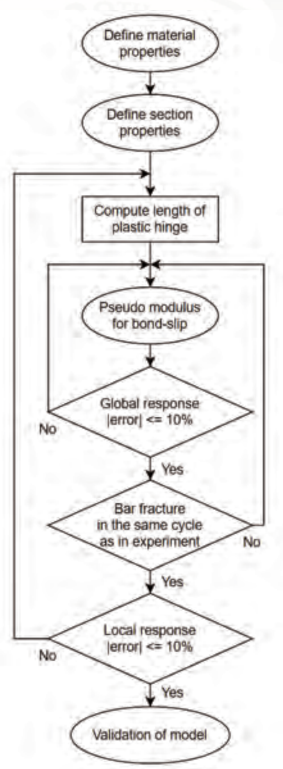

Concrete Model

- Mander's model characterized concrete with two distinct properties: core concrete and cover concrete.
- The unconfined or cover concrete parameters were determined using the compressive strength obtained from a cylinder compression test.
- The *UniaxialMaterial Concrete04* material model, available in OpenSees, was utilized to numerically model properties derived from Mander's model.
- For columns with externally wrapped CFRP, the cover concrete is now confined due to the confinement effect of CFRP wraps.
- The compressive strength of the concrete was determined to be 55 MPa for the columns based on cylinder tests

Concrete Model

- Unconfined Concrete:
  - f'_{cc} = 8 ksi
  - ε_{cc} = 0.0022
  - ε_{cu} = 0.005
- Confined Concrete:
  - f'_{cc} = 12.85 ksi
  - ε_{cc} = 0.0087
  - ε_{cu} = 0.0206
- CFRP Confined Concrete:
  - f'_{cc} = 15.24 ksi
  - ε_{cc} = 0.012
  - ε_{cu} = 0.0285

- FRP Confinement (Sankholkar et al. 2018):

$$f'_{cc} = f'_{co} + 1.31 f_l$$

$$\varepsilon_{ccu} = \varepsilon'_c \left(2.4 + 5.6 \frac{f_l}{f'_{co}} \left(\frac{\varepsilon_{h,rup}}{\varepsilon'_c} \right)^{0.15} \right)$$

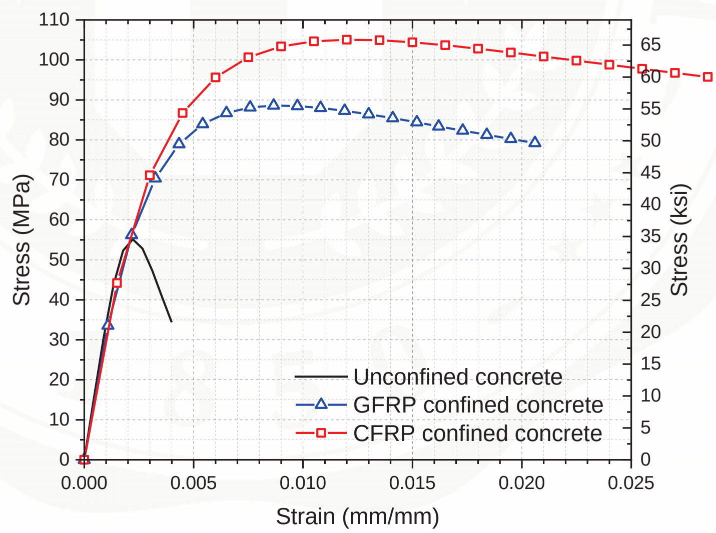

Bond-Slip Effects: Pseudo Reinforcing Bars

- Bar slippage results in a softer global response.
- A pseudo-reinforcing bar is used within the plastic hinge zone.

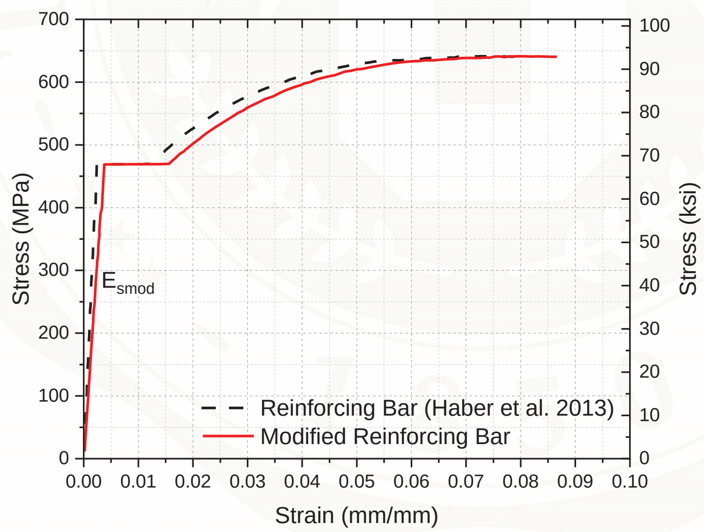

Low-Cycle Fatigue Bar Fracture

- Test columns failed due to low-cycle fatigue bar fracture of steel bar.
- Exemption happened for the HYB column (No-PT) when a GFRP bar fractured.
- Coffin-Manson expression with cumulative linear damage rule:

$$\varepsilon^p = C_f(2N_f)^{-\alpha}$$

$$D_f = \frac{1}{\sum_{i=1}^{n}(2N_f)_i}$$

- *ReinforcingSteel* material in OpenSees is capable of predicting low-cycle fatigue life of rebar.

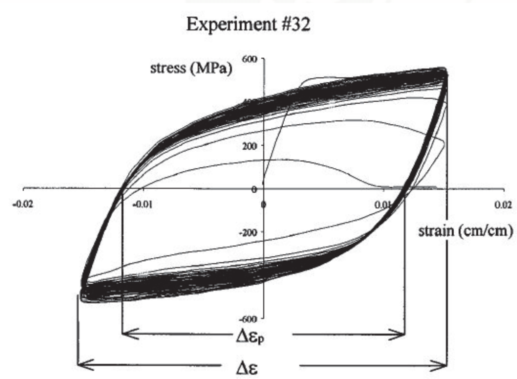

Source: Brown and Kunnath, 2000

GFRP Bar Model

- The material model for GFRP bars is modeled as a bilinear elastic material.
- The GFRP bar was modeled bilinear as *ElasticBilin* material since geometrical non-linearity arose in the GFRP bars due to the column bending and increasing curvature.
- Notably, instead of linear with one elastic slope, the GFRP bars were modeled as bi-linear with two different slopes calibrated with the experiments until they matched and applied for all hybrid longitudinal configurations.

GFRP Bar Model

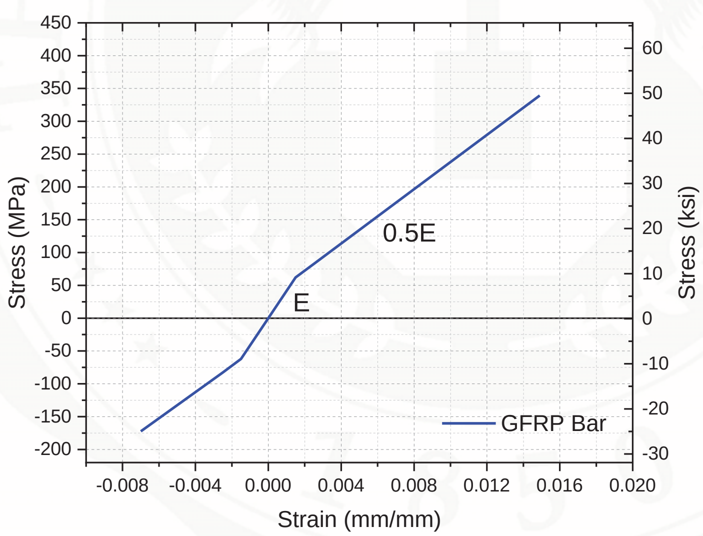

PT Bar Model

- The *UniaxialMaterial Steel4* defines tensile stress-strain behavior for threaded PT bars with initial stress accommodation.
- Isotropic hardening is excluded due to non-uniform yield surface expansion post-yield stress.
- The *corotTrussElement* was used to model the post-tensioning bars with *Steel04* material properties.
- The *corotTrussElement* considers the non-linear geometry of the material that occurs during the bending of the column.

PT Bar Model

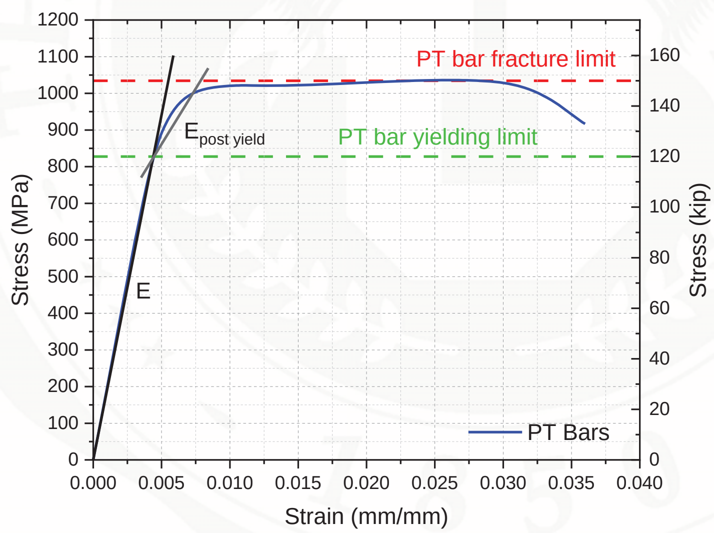

Layout of Proposed Model

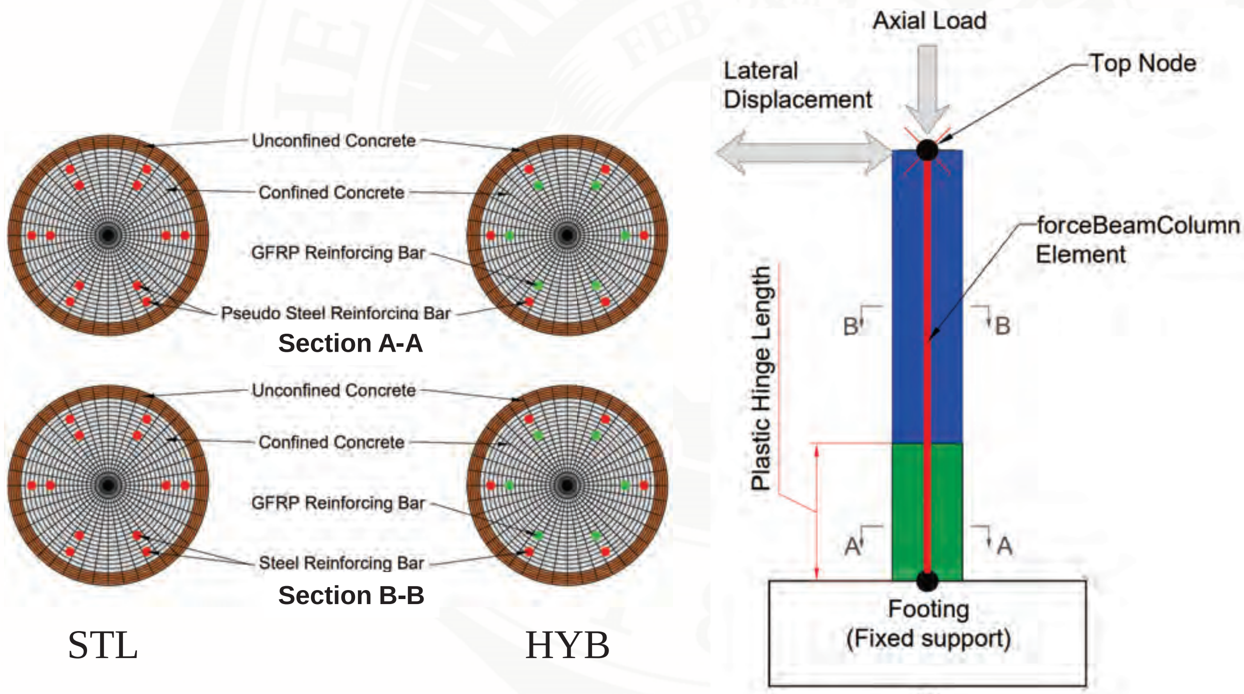

Non-PT Columns

Layout of Proposed Model

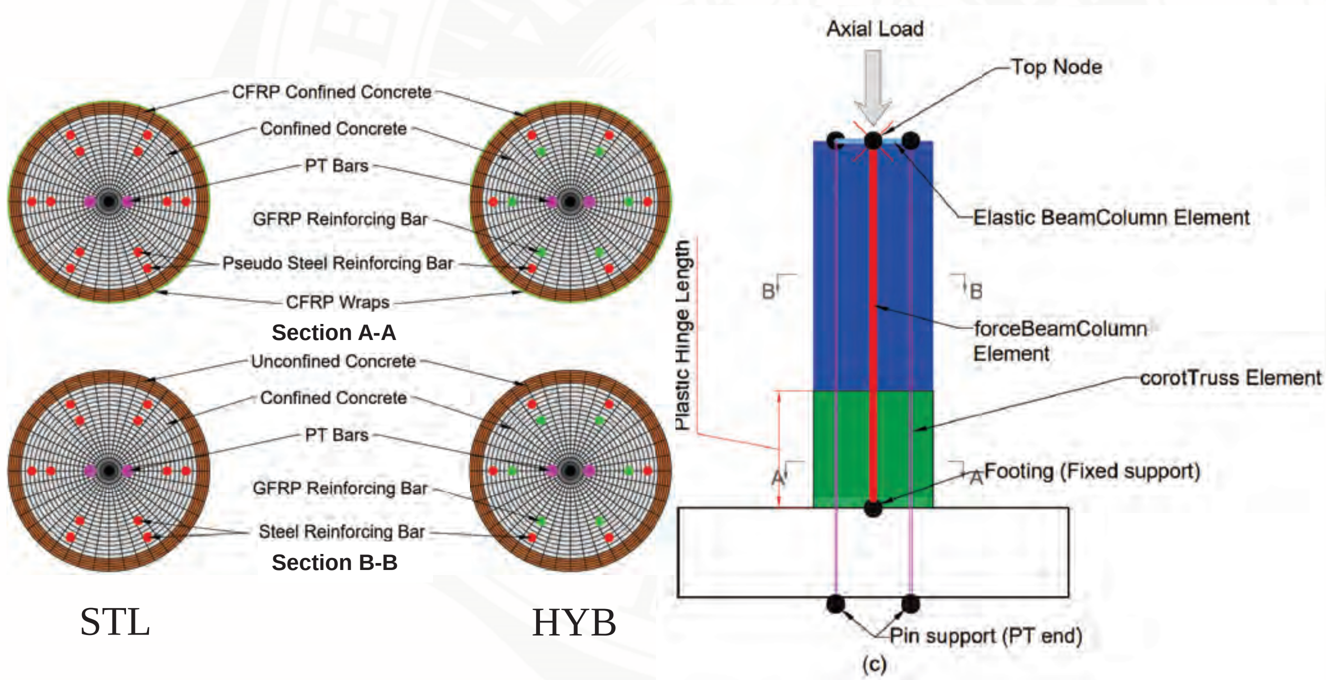

PT Columns

Validation of Global Response

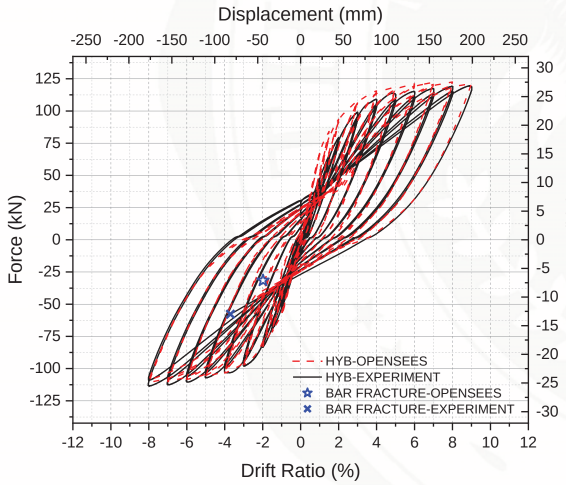

HYB

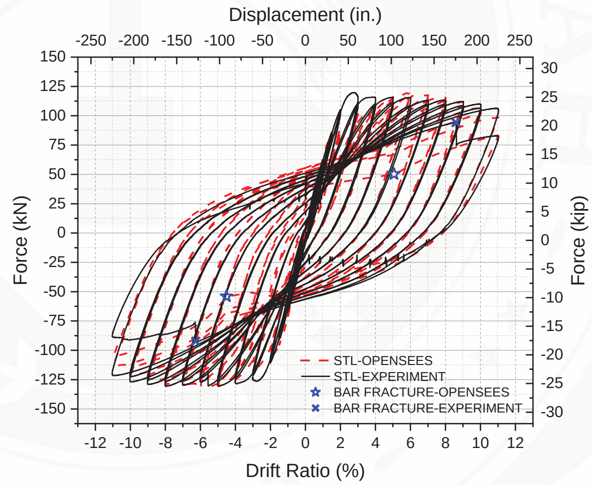

STL

Non-PT Columns

Validation of Global Response

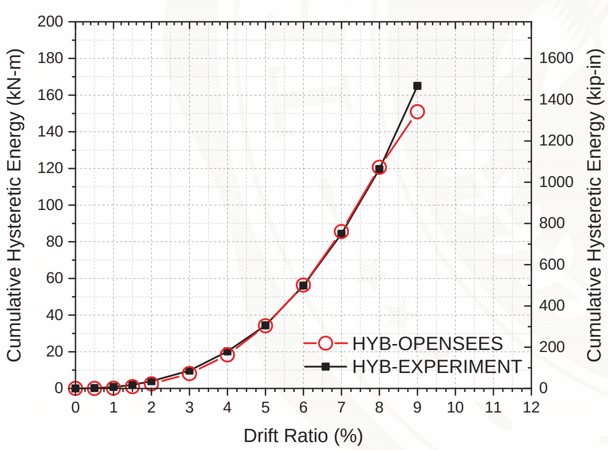

HYB

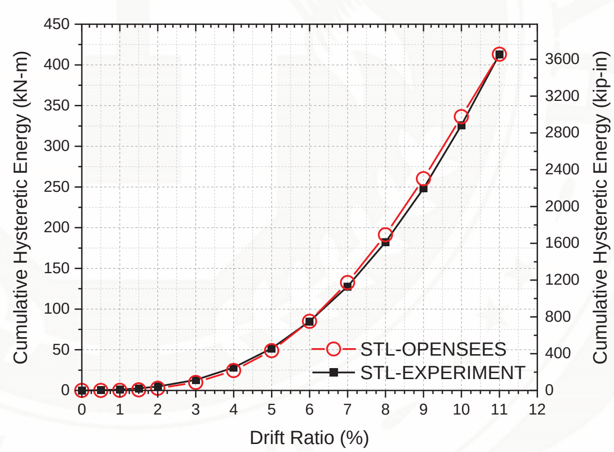

STL

Non-PT Columns

Introduction | Proposed Research | Pull-out Test | Non-PT Tests | PT Tests | Numerical Study

Validation of Global Response

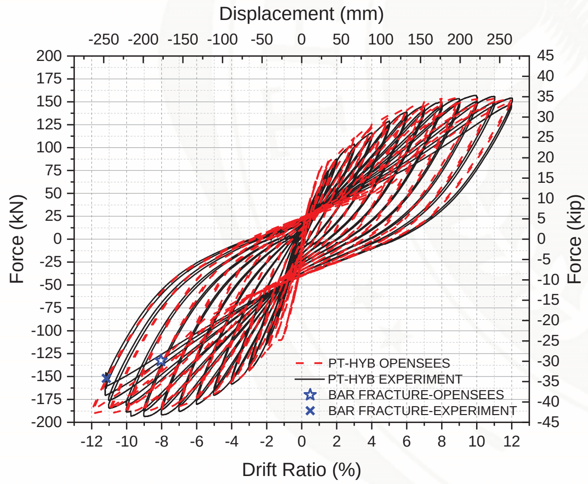

HYB

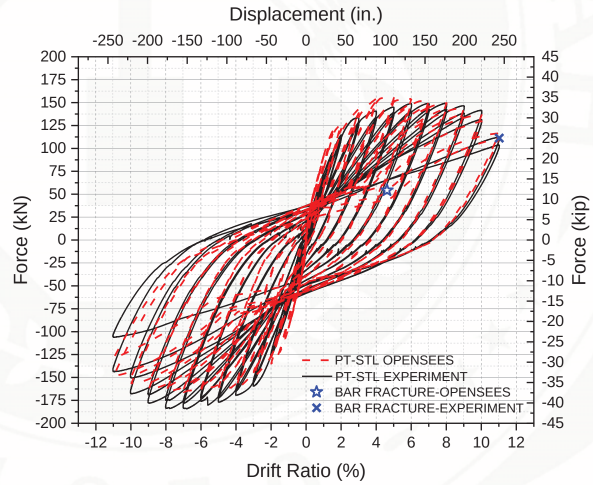

STL

PT Columns

Validation of Global Response

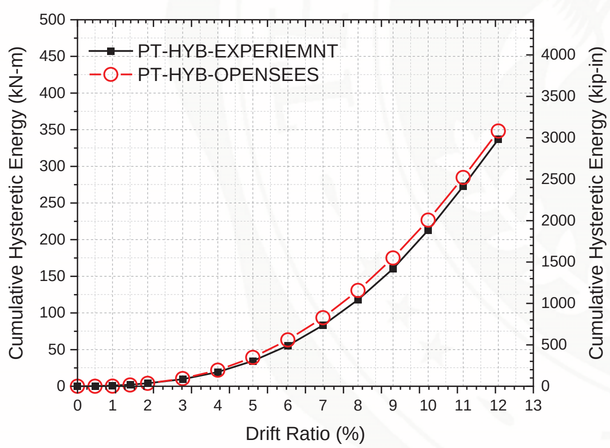

HYB

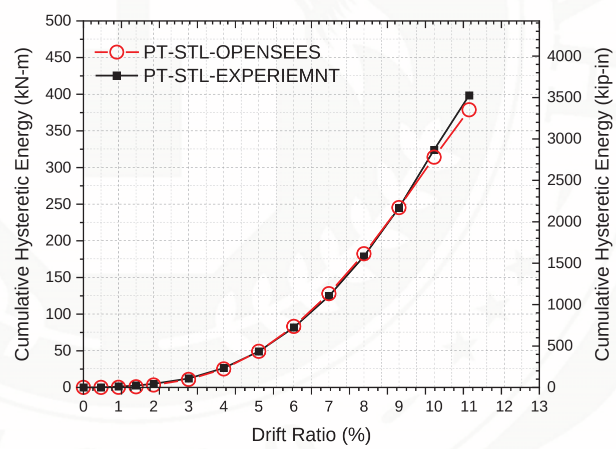

STL

PT Columns

Validation of Local Response

- The local response of the numerical models was assessed based on the drift ratio at which bar fracture occurred.
- In the experiment of non-PT columns, HYB column and STL column witnessed the fracture of longitudinal bars during the 9.0% and 11.0% drift ratio, respectively.
- Regarding PT columns, the experiment recorded bar fractures of HYB and STL columns at 11.0%.
- The numerical model predicted bar fracture at the same drift ratio as the experimental study. The failure in the numerical model occurred at the same cycle as in the experimental study.

Validation of Local Response

- The numerical model predicted the PT bar distribution; the loading and unloading curves are in good agreement with the experimental results.
- Both columns observed a difference of less than 5.0% of the peak PT force between the model and experimental results.
- It is also indicated that none of the PT bars reached the yielding limit.
- For HYB column, the gap of push cycles of the west PT bars can be justified by the initially progressive concrete spalling above the CFRP-wrapped region, resulting in lower PT force in the experiment than the model. On the other hand, the east PT bar in STL column dug into the concrete at the top column and caused a gap in the push cycles.

Validation of Local Response – PT Forces

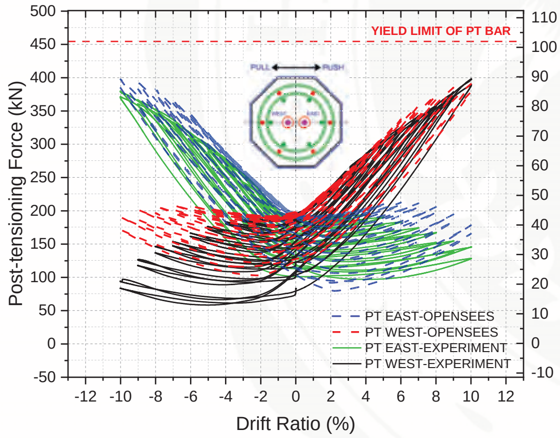

HYB

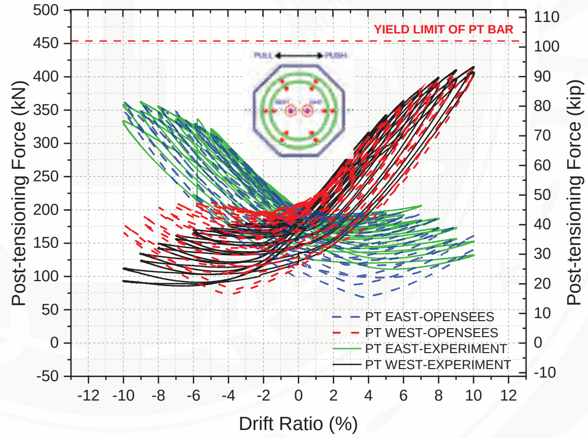

STL

Conclusions

- The beam-column element used in the numerical model, incorporating plastic hinge length, buckling, and low cycle fatigue of intentionally debonded reinforcing bars, effectively represents actual behavior under cyclic loading.
- It predicts the response of the precast column with grouted ducts satisfactorily in both global and local levels.
- Confined concrete, steel/GFRP bars, and PT bar models proposed in the numerical models proved their effectiveness in building the model to calibrate the column tests.

Conclusions

- The impact of reinforcing bar bond-slip and debonding can be accurately predicted by the models presented in this paper, along with the modified material properties of the plastic hinge region.
- Therefore, the proposed numerical model effectively models precast-reinforced concrete members.
- All models accurately predicted a column's maximum quasi-cyclic drift ratio before a bar fracture happens: 9.0% for HYB, 11.0% for STL, 12.0% for PT-HYB and PT-STL columns. These drift ratios exceed the limits suggested by seismic design codes, indicating that the intentional debonding details of reinforcing bars can be utilized in seismic zones

TRANSPORTATION LEARNING NETWORK

A partnership with MDT•NDDOT•SDDOT•WYDOT and the Mountain-Plains Consortium Universities

Thank you for participating!

Please take a moment to complete the evaluation included in the reminder email.

We appreciate your feedback.

Contact Information

Chris Padilla
chris.padilla@ndsu.edu
(701) 202-5730

Susan Hendrickson
susan.Hendrickson@ndsu.edu
(701) 238-8646

Shannon Olson
shannon.l.olson@ndsu.edu
(701) 552-0672

Amanda Miller
amanda.jean.miller@ndsu.edu

https://tln.learnflex.net
https://www.translearning.org

Thank you to our partners:

MOUNTAIN-PLAINS CONSORTIUM · MONTANA MDT DEPARTMENT OF TRANSPORTATION · NORTH Dakota Be Legendary. | Transportation · SD DEPARTMENT OF TRANSPORTATION · WYOMING TRANSPORTATION DEPARTMENT